

ICE THICKNESS AND BED CONDITIONS OF THE NORTH EAST GREENLAND ICE STREAM

INTRODUCTION

The Greenland ice sheet is a key area for rapid ice mass changes and future implications for ice sheet mass balance and sea level contribution (Tapley and others, 2019; Masson-Delmotte and others, 2018; Kjær and others, 2013). A prominent feature of the Greenland ice sheet is the North East Greenland Ice Stream (NEGIS, Figure 1). This 600- km-long ice stream drains 12% of the Greenland ice mass via fast-flowing marine-terminating outlet glaciers (Larsen and others, 2018).

Here, we provide a high resolution ice thickness data set derived from a radio echo sounding survey of a large part of NEGIS in the vicinity of EGRIP drill site (Figure 2). The computation of a detailed bedrock elevation model for the region allows us to study flow related features of the ice stream and link them to ice thickness and topography.

DATA

The data has been recorded in May 2018 with AWI's ultra-wideband multi-channel radar installed on the AWI Polar6 Basler BT-67 aircraft (Figure 4).

- Number of channels: 8
- Mapped area: 24000 km² (8233 km of profiles)
- Grid spacing: 5 – 10 km
- ~ 150 km up- and downstream of EGRIP drill site

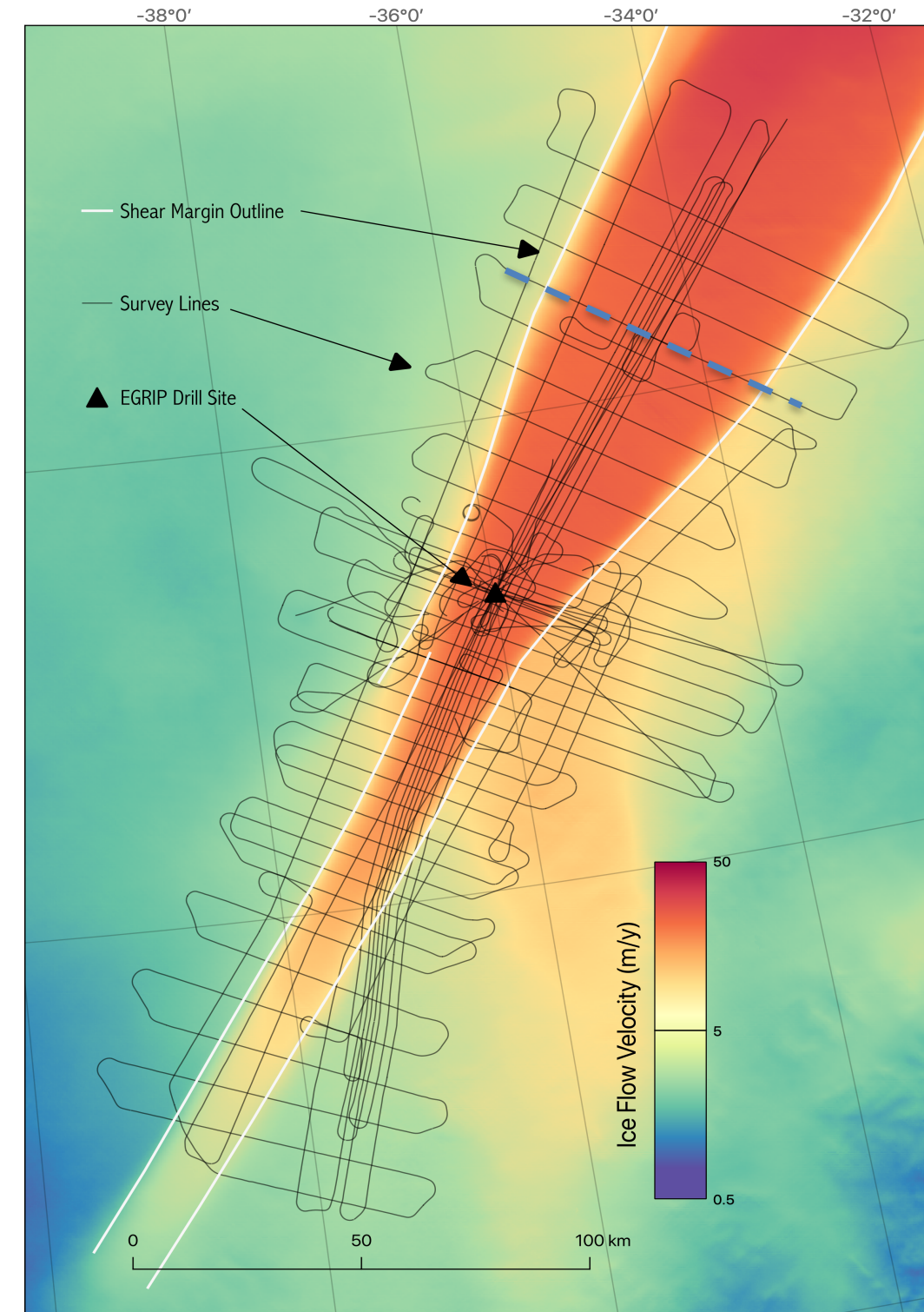


Figure 2: Ice sheet velocity field (Joughin and others 2018) of the survey area from the UWB campaign on the North East Greenland Ice Stream (NEGIS). The survey lines extend 150 km up and downstream of the EGRIP drill site and over the shear margins. Survey lines upstream from the EGRIP drill site have a spacing of 5 km and further up- and downstream 10 km spacing. The dashed blue line represents the profile in Figure 6.

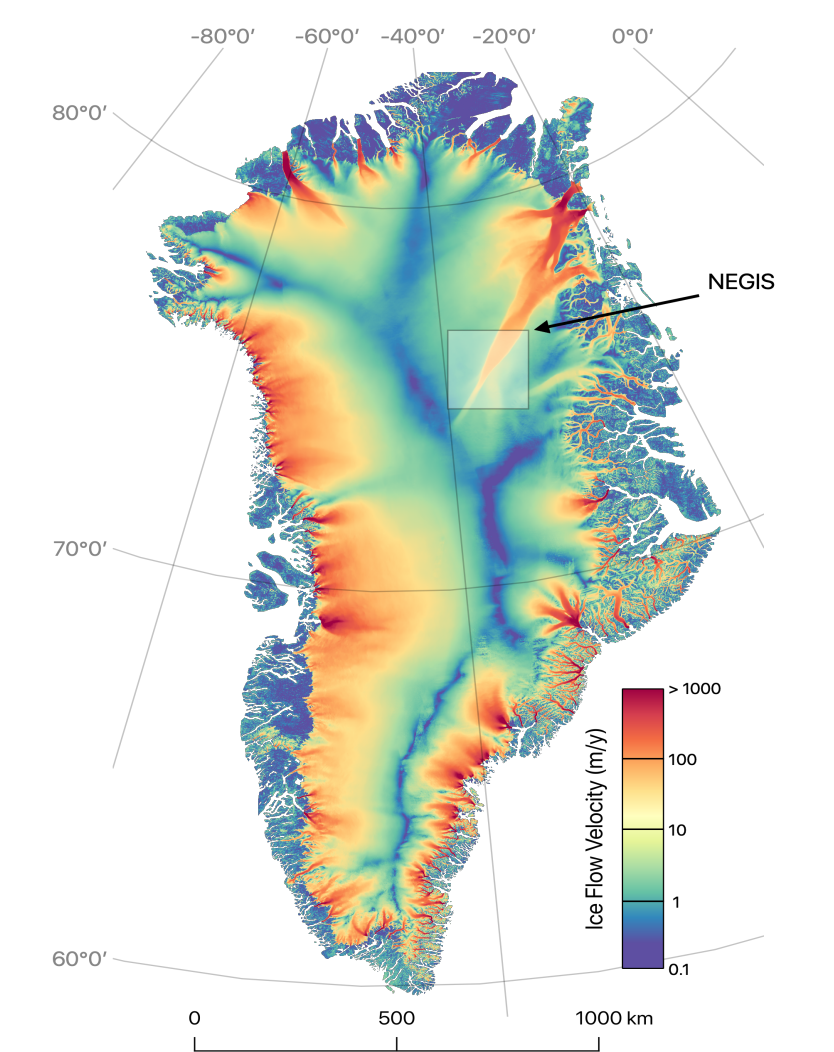


Figure 1: Map of the velocity profile of the Greenland Ice Sheet (Joughin and others 2018). The survey area is marked with a white outline.

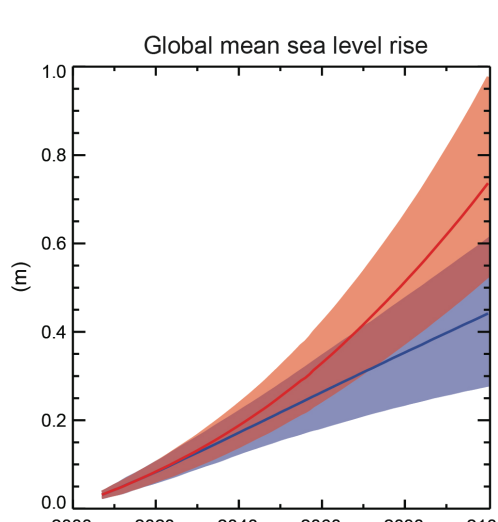


Figure 3: Modelled global mean sea level rise over the 21st century relative to 1986-2005, derived from a combination of the CMIP5 ensemble with process-based models, for RCP2.6 and RCP8.5 (Church and others, 2013).



Figure 4: AWI's Polar6 aircraft in Antarctica 2019 with the UWB antenna mounted underneath the fuselage (Image: Steven Franke).

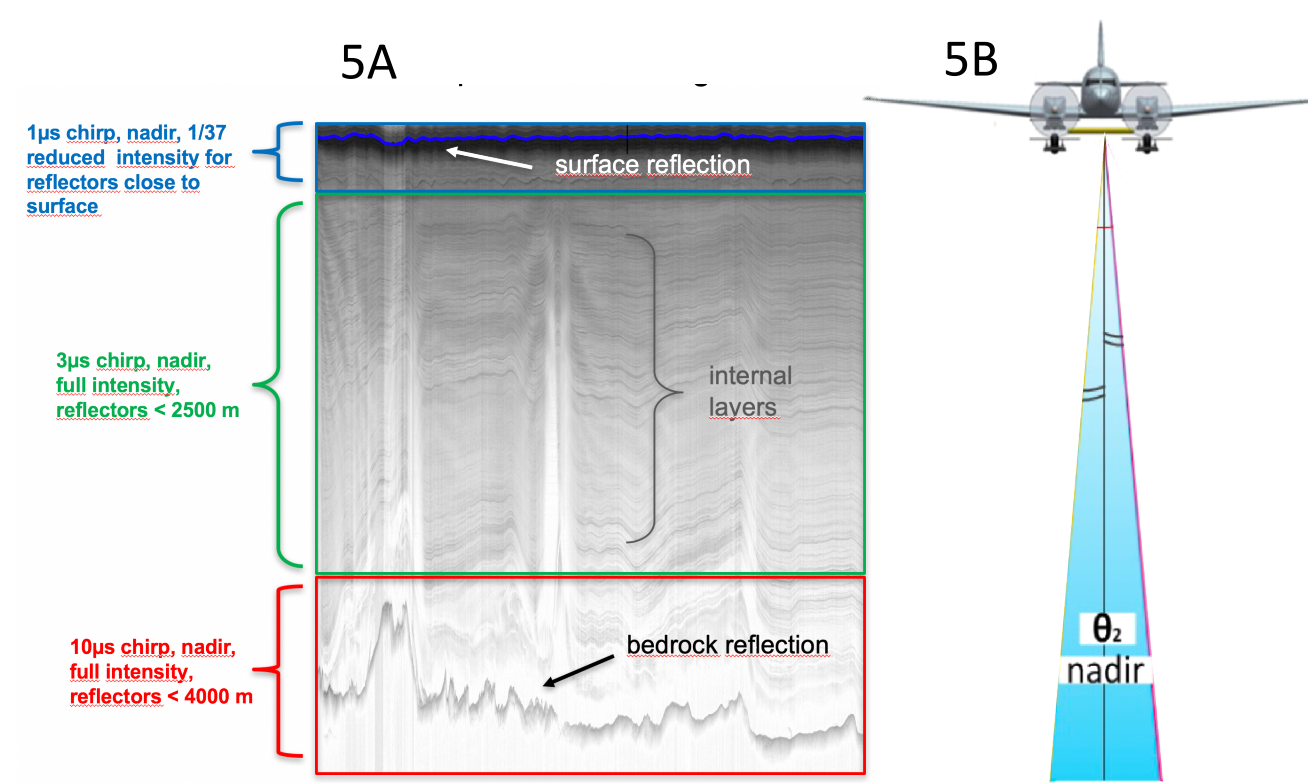


Figure 5: Schematic illustration of the waveform transmission. Three linear chirp pulses are emitted to sound different parts of the ice sheets (SA). The radar signal is steered towards nadir (SB, modified from Hale and others 2016).

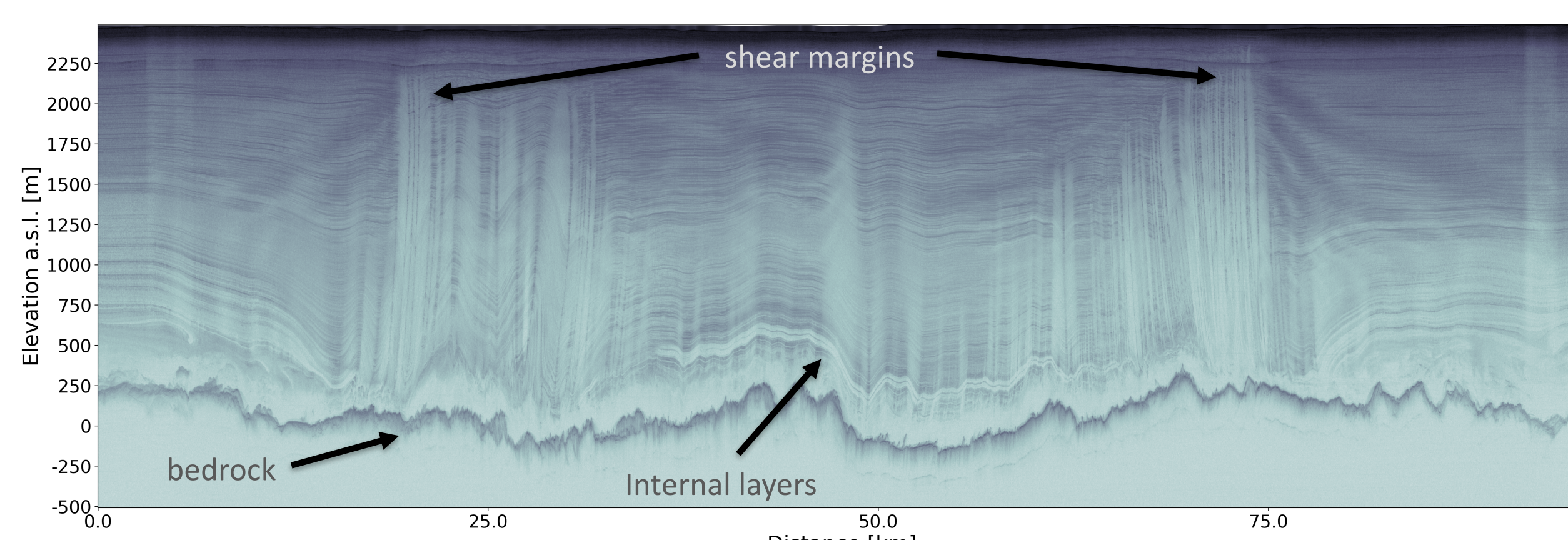


Figure 6: Echogram of a profile vertical to ice flow direction. Both shear margins are represented as well as internal reflections and the basal reflector. The section is represented in Figure 2 as a blue dashed line.

Table 1: Overview of the radar data set and acquisition parameters.

Parameter	Value
Collected Raw Data	12 TB
Total survey length	8233 km
Frequency Range	180 – 210 MHz
Waveform Signals	1µs, 3µs, 10µs chirp
Pulse Repetition Frequency	10 kHz
Tukey Window	0.8
Flight Altitude	1200 ft
Aircraft Velocity	160 mph

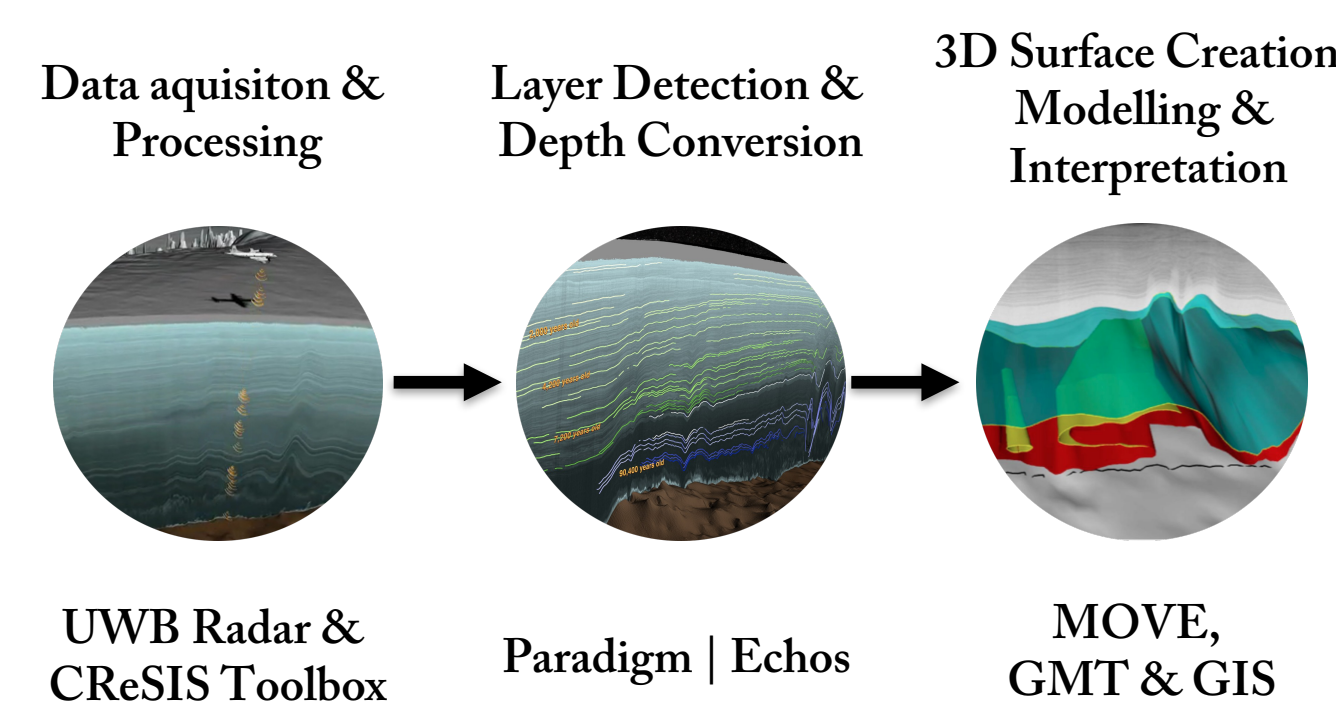


Figure 7: Workflow for UWB radar data. Data recording is performed with the UWB system on Polar6 aircraft. Radar data processing is performed with the CREGIS Toolbox on AWI's HPC Cray high performance computer. Reflection layers are detected with the Paradigm – ECHOS software suite and 3D surfaces are created with software like MOVE, GMT, GIS systems among others.

RADAR SYSTEM

Since 2016 the German Alfred Wegener Institute (AWI) has been operating a multi-channel ultra-wideband (UWB) air-borne radar sounder and imager for sounding ice thickness, imaging internal layering and the ice-bedrock interface of polar ice sheets. The radar system is installed on the AWI Polar6 Basler BT-67 aircraft (Figure 4).

Eight power amplifiers enable a maximum transmit power of 1000 W peak power. A variable gain stage can be set for each analog receiver channel as well as an anti-aliasing band-pass filter (Hale and others, 2016). The radar system is also able to alternate between different pulse length stages and different receiver gains for each stage to increase the dynamic range.

METHODS

Our sketch of our workflow is represented in Figure 7. For our radar data processing we use the CREGIS Toolbox algorithms for all three domains in along-track (f-k migration), cross track (array processing) and vertical component (pulse compression).

Radar data is recorded in the time domain and converted into depth. On behalf of our surface and bedrock detection, we calculate the thickness of the ice column for every trace and derive the bedrock elevation. We also computed surface slopes on the basis of the Arctic DEM model (Porter and others, 2018) and compared major elevation changes with our bedrock.

RESULTS

We derived the ice thickness and created a bedrock model nested into the bedrock topography of Morlighem and others (2017) BedMachine v3 (BMv3).

Ice thickness and Bedrock Elevation

- Ice thickness increases towards downstream from 2059-3092 m
- Variations dominated by topography which ranges from -293 to 606 m

Main Findings

1. Location of an elevation difference of up to 367 m
2. A hill that is not present in our data, but a folded region with a strong internal reflection
3. A ridge in the central northern part that of the survey area
4. Next to the ridge, we find a trough with steep slopes
5. Isolated bedrock undulations

Furthermore, surface elevation changes correlate with bedrock features in respect to ice flow direction and to the position of the shear margin (Figure 10).

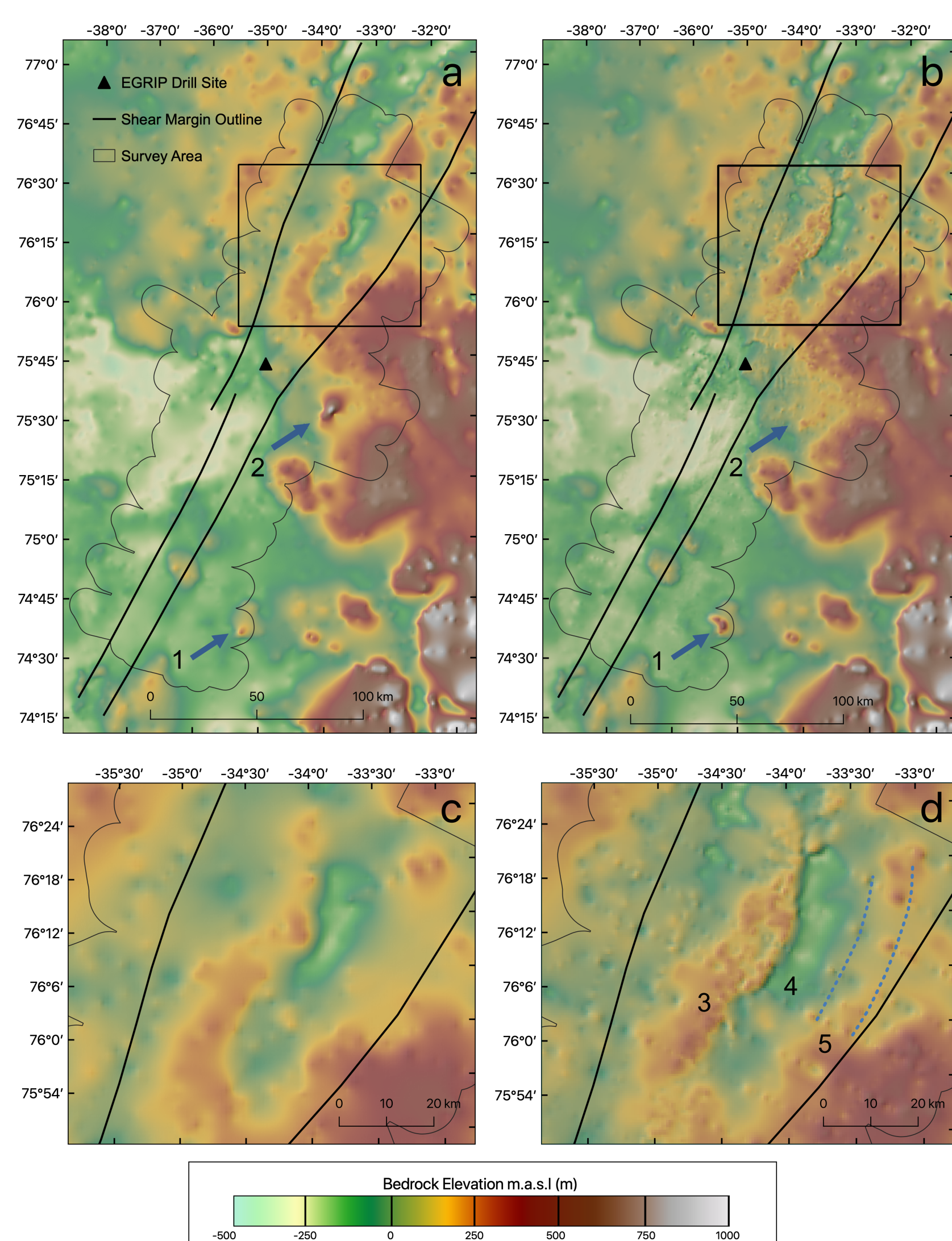


Figure 8: Bedrock topography of BedMachine v3 (Morlighem and others (2017), a) and bedrock derived from our ice thickness data (b). A close-up for the area upstream of the EGRIP drill site for both models is shown on the two upper images marked with a blue outline (c and d). Two locations with strong elevation differences are marked with a blue arrow. In the zoom section c and d we show the location of feature 3-5.

DISCUSSION

The bedrock reflection is sometimes masked by internal reflections, representing basal entrainments and by steep dipping reflectors. Large surface elevation changes are correlated with the ice streaming over bedrock bumps and get more frequent in downstream (Figure 10). Moreover, we interpret off-nadir reflectors as ridges extending in ice flow direction.

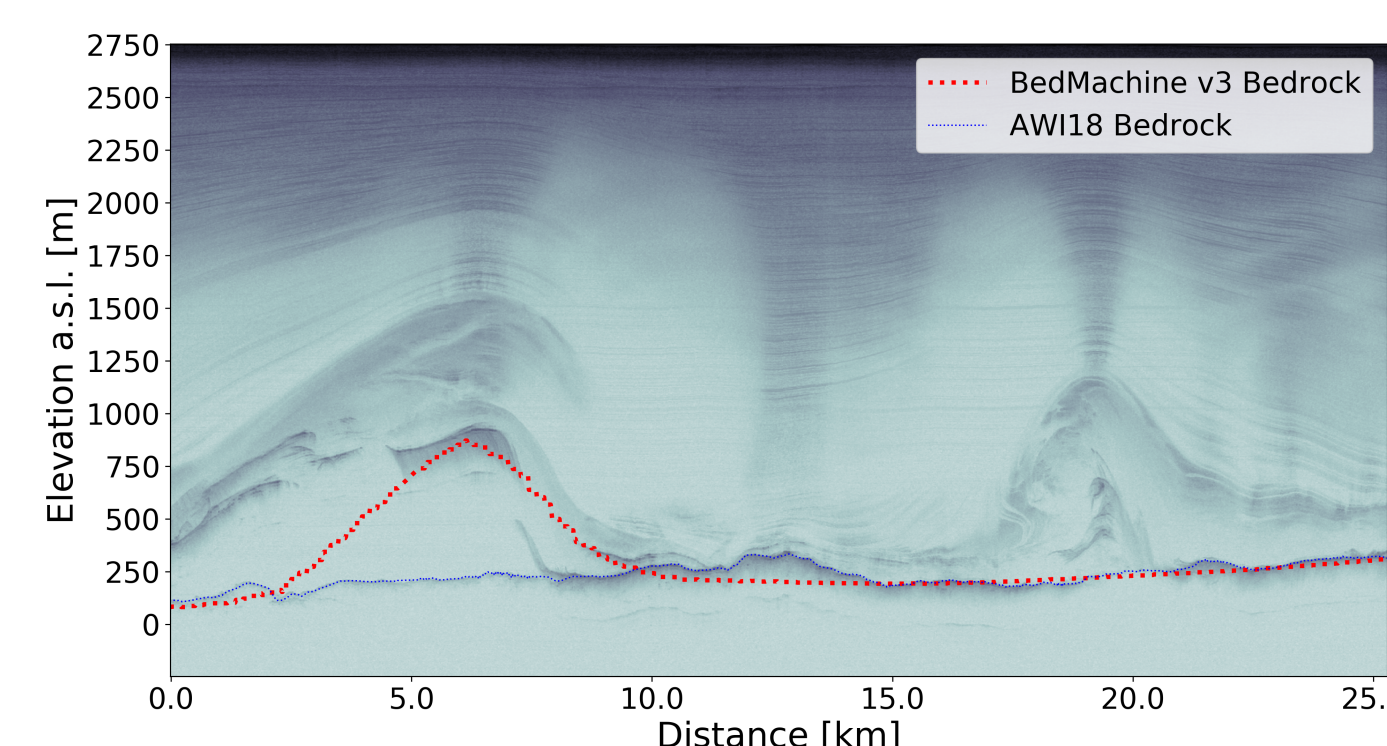


Figure 9: Echogram from a profile along the point of our highest deviation in ice thickness (Number 2 in Figure 8 a and b). The dashed red line represents the bedrock elevation as used in BedMachine v3 (Morlighem and others, 2017). The high peak at 12 km distance of the profile and 0 750 m elevation correlates with a high energy reflector located in a folded area. Underneath that undulation a fainter coherent reflection with a lower amplitude is visible, which we interpret as the bedrock reflection.

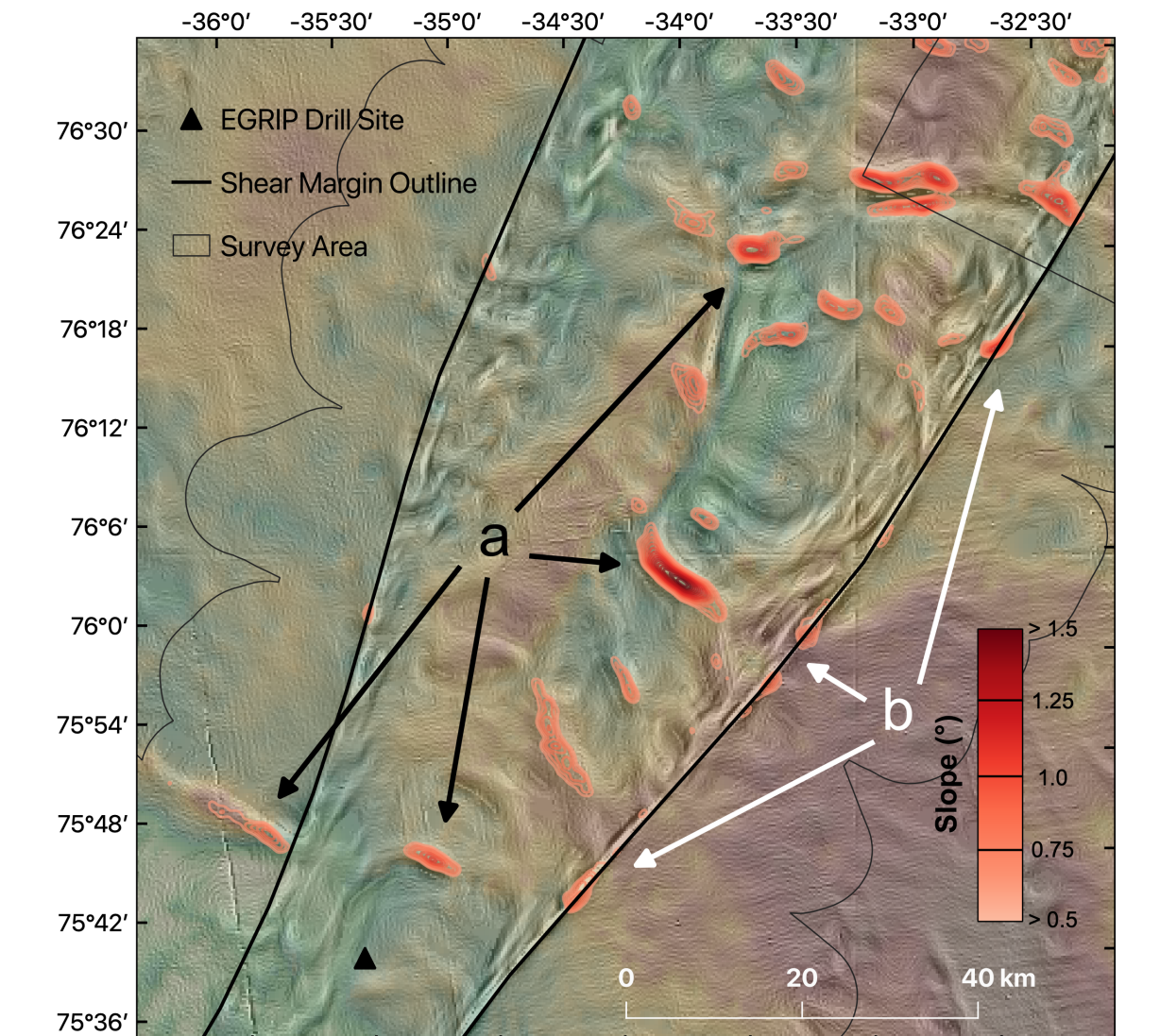


Figure 10: Bedrock topography and major changes in surface elevation (slopes higher than 0.65°) represented with reddish contour lines. Two slope related systems could be identified: (1) bedrock topography related marked as a, (2) shear margin related features marked as b. Slope and curvature were derived from the Arctic DEM surface elevation model (Porter and others, 2018).

CONCLUSIONS

For future sea level projections it is important to understand the ice dynamics of ice streams like NEGIS. One important key feature is to understand ice flow properties and the effect of bedrock topography in this context.

Our detailed bedrock topography shows new and more detailed structures with potential implications for basal water routing as well as traces of current and past ice dynamics.

ACKNOWLEDGEMENTS

This work was funded by AWI's strategy fund. We thank the crew of the research aircraft Polar 6. Logistical support was provided by the East Greenland Ice-Core Project. We acknowledge the use of software from CREGIS generated with support from the State of Kansas, NASA Operation IceBridge grant NN16AH54G, and NSF grant ACI-1443054. Furthermore, we acknowledge the use of Paradigm by Emerson E&P Software.

REFERENCES

Hale and others (2016) MULTI-CHANNEL ULTRA-WIDEBAND RADAR SOUNDER AND IMAGER Center for Remote Sensing of Ice Sheets, University of Kansas Alfred Wegener Institute, Germany, 2016
IEEE International Geoscience and Remote Sensing Symposium (IGARSS)
Joughin and others (2018) A complete map of Greenland ice velocity derived from satellite data collected over 20 years. *Journal of Glaciology*, 64(243), 1–11, ISSN 0022-1430 (doi:10.1017/jglu.2017.273)
Kjær and others (2013) Aerial Photogrammetry Reveals Late-20th-Century Dynamic Ice Loss in Northwestern Greenland. *Science*, 337(October), 569–574
Masson-Delmotte and others (2018) Global warming of 1.5°C. An IPCC Special Report, volume 265. ISBN 9789291691517
Morlighem and others (2017) BedMachine v3: Complete Bed Topography and Ocean Bathymetry Mapping of Greenland From Multibeam Echo Sounding Combined With Mass Conservation. *Geophysical Research Letters*, 44(21), 11451–11461, ISSN 1542-0275 (doi:10.1002/2017GL074914)
Porter and others (2018) Arctic DEM: Arctic DEM (doi:10.7927/H7J9H1H3H1)
Riegler-Morales and others (2014) Advanced multidimensional radar instrumentation for polar research. *IEEE Transactions on Geo- science and Remote Sensing*, 52(7), 2824–2842, ISSN 0192-9292 (doi:10.1109/TGRS.2013.2266445)
Tapley and others (2019) Contributions of GRACE to understanding climate change. *Nature Climate Change*, ISSN 1758-0798 (doi:10.1038/s41558-019-0456-2)